Carbohydrate Polymers 259 (2021) 117781

Contents lists available at ScienceDirect

Carbohydrate Polymers

journal homepage: www.elsevier.com/locate/carbpol

TEMPO/$NaClO_2$/NaOCl oxidation of arabinoxylans

Carolina O. Pandeirada [a], Donny W.H. Merkx [a,b], Hans-Gerd Janssen [b,c], Yvonne Westphal [b], Henk A. Schols [a,*]

[a] Wageningen University & Research, Laboratory of Food Chemistry, P.O. Box 17, 6700 AA Wageningen, the Netherlands
[b] Unilever Foods Innovation Centre – Hive, Bronland 14, 6708 WH Wageningen, the Netherlands
[c] Wageningen University & Research, Laboratory of Organic Chemistry, P.O. Box 8026, 6700 EG Wageningen, the Netherlands

ARTICLE INFO

Keywords:
Arabinoxylan
TEMPO-oxidation
Arabinuronoxylan
Arabinuronic acid

ABSTRACT

TEMPO-oxidation of neutral polysaccharides has been used to obtain polyuronides displaying improved functional properties. Although arabinoxylans (AX) from different sources may yield polyuronides with diverse properties due to their variable arabinose (Ara*f*) substitution patterns, information of the TEMPO-oxidation of AX on its structure remains scarce. We oxidized AX using various TEMPO:$NaClO_2$:NaOCl ratios. A TEMPO:$NaClO_2$:NaOCl ratio of 1.0:2.6:0.4 per mol of Ara gave an oxidized-AX with high molecular weight, minimal effect on xylose appearance, and comprising charged side chains. Although NMR analyses unveiled arabinuronic acid (AraA*f*) as the only oxidation product in the oxidized-AX, accurate AraA quantification is still challenging. Linkage analysis showed that > 75 % of the β-(1→4)-xylan backbone remained single-substituted at position *O*-3 of Xyl similarly to native AX. TEMPO-oxidation of AX can be considered a promising approach to obtain arabinuronoxylans with a substitution pattern resembling its parental AX.

1. Introduction

Modification of neutral polysaccharides to anionic polymers by the generation of polyuronides may lead to improved/unique functional properties of the polymer (Pierre et al., 2017). For example, these polyuronides can show thickening and gelling properties, similarly to pectin, a naturally occurring polyuronide (Sundar Raj, Rubila, Jayabalan, & Ranganathan, 2012). Additionally, conversion of neutral polysaccharides to polyuronides has also enabled the production of nano-fibres (Habibi, 2014; Meng, Fu, & Lucia, 2016) compatible with biomedical applications (Chao et al., 2019).

2,2,6,6-tetramethylpiperidine-1-oxyl radical (TEMPO)-mediated oxidation is one of the major approaches used to selectively oxidize primary hydroxyl groups of neutral polysaccharides into carboxylic acids to obtain polyuronides (Bragd, Van Bekkum, & Besemer, 2004; de Nooy, Besemer, & van Bekkum, 1995; Hao et al., 2020; Isogai, Hänninen, Fujisawa, & Saito, 2018; Pierre et al., 2017; Tamura, Wada, & Isogai, 2009). A TEMPO/NaOCl/NaBr system at pH 10 was the first system used to convert C6 primary hydroxyls to carboxyl groups in the neutral polysaccharides starch and inulin (de Nooy, Besemer, & van Bekkum, 1994), and it is still the most used condition set to oxidize polysaccharides (Pierre et al., 2017). However, the alkaline medium used in the TEMPO/NaOCl/NaBr system can lead to undesirable polysaccharide depolymerization (Spier, Sierakowski, Reed, & de Freitas, 2017). This depolymerization can be overcome by using alternative systems that do not require the use of an alkaline medium, such as

Abbreviations: AX, arabinoxylan; AraA*f*, arabinuronic acid; BAIB, bis(acetoxy)iodobenzene; COSY, homonuclear ^{1}H-^{1}H correlation spectroscopy; DB, degree of branching; DO, degree of oxidation; EI, impact mode; GC–MS, gas chromatography coupled to mass spectrometry; HILIC, hydrophilic interaction chromatography; HPAEC-PAD, High-Performance Anion-Exchange Chromatography with Pulsed Amperometric Detection; HPSEC, high performance size exclusion chromatography; Hydr_ox-AX$^{1.0:2.6:0.4}$_H_2O, water fraction collected by SPE of the hydrolysate ox-AX$^{1.0:2.6:0.4}$; Hydr_ox-AX$^{1.0:2.6:0.4}$_TFA, acetronitrile:water 60:40, containing 0.05 % (v/v) TFA fraction collected by SPE of the hydrolysate ox-AX$^{1.0:2.6:0.4}$; IS, internal standard; I_{sugar}, ^{1}H-NMR signal integrals derived from each identified sugar; MS, mass spectrometry; Mw, molecular weight; $NaBD_4$, sodium borodeuteride; $NaClO_2$, sodium chlorite; NaOCl, sodium hypochlorite; ox-AX, oxidized-AX; ox-AX$^{1.0:2.6:1.5}$, oxidized-AX with a TEMPO:$NaClO_2$:NaOCl ratio of 1.0:2.6:1.5 per mol of C5-OH of Ara; ox-AX$^{0.2:2.6:1.5}$, oxidized-AX with a TEMPO:$NaClO_2$:NaOCl ratio of 0.2:2.6:1.5 per mol of C5-OH of Ara; ox-AX$^{1.0:2.6:0.4}$, oxidized-AX with a TEMPO:$NaClO_2$:NaOCl ratio of 1.0:2.6:0.4 per mol of C5-OH of Ara; ox-product, oxidized-product; PMAA, partially methylated alditol acetate; Red-ox-AX$^{1.0:2.6:0.4}$, carboxyl-reduced ox-AX$^{1.0:2.6:0.4}$ with carbodiimide/$NaBD_4$; SG, switchgrass; SPE, solid phase extraction; TEMPO, 2,2,6,6-tetramethylpiperidine-1-oxyl radical.

* Corresponding author.
E-mail address: henk.schols@wur.nl (H.A. Schols).

https://doi.org/10.1016/j.carbpol.2021.117781
Received 20 November 2020; Received in revised form 4 February 2021; Accepted 4 February 2021
Available online 9 February 2021

TEMPO/bis(acetoxy)iodobenzene (BAIB) in an acetonitrile-aqueous buffer mixture (Börjesson & Westman, 2016; Chatterjee et al., 2017; Tojo & Fernández, 2007) or TEMPO/NaOCl/$NaClO_2$ (sodium chlorite) in a mild acidic (pH 3.5–6.8) medium (Hao et al., 2020; Saito, Hirota, Tamura, & Isogai, 2010; Tamura et al., 2009; Tamura, Hirota, Saito, & Isogai, 2010; Tanaka, Saito, & Isogai, 2012).

TEMPO-oxidation has been mostly performed on neutral polysaccharides composed of hexoses, such as cellulose (Mendoza, Browne, Raghuwanshi, Simon, & Garnier, 2019; Meng et al., 2016), starch (Hao et al., 2020), galactomannans (Sakakibara, Sierakowski, Lucyszyn, & de Freitas, 2016; Sierakowski, Milas, Desbrières, & Rinaudo, 2000), and curdlan (Tamura et al., 2010). Although not many studies have been performed on TEMPO-oxidation of pentose-based polysaccharides (pentosans), arabinoxylan (AX), a major hemicellulose of the cereal cell walls (Izydorczyk, 2009), is a promising pentosan to obtain polyuronides. Arabinoxylans are composed of a linear β-(1→4)-xylan backbone mainly substituted with single α-L-Ara*f* units, which are attached at positions *O*-3 and/or *O*-2 of the β-D-Xyl*p* unit (Perlin, 1951). As the primary hydroxyl groups in the AX structure are only shown in the C5 position of the Ara*f* units (Perez, 2018), TEMPO-oxidation of an AX would selectively oxidize the Ara*f* side chains to arabinuronic acid (AraA*f*), keeping the β-(1→4)-xylan backbone intact and creating a polyuronide (arabinuronoxylan) carrying negative charged sugar residues as side chains. As the level and distribution of the Ara*f* side chains along the xylan backbone can differ among arabinoxylans from different sources (Izydorczyk & Biliaderis, 1995), TEMPO-oxidation of various arabinoxylans might yield arabinuronoxylans with a wide range of different properties, which can be valuable for food and/or biomedical applications.

Parikka et al. (2017) and Börjesson and Westman (2016) oxidized an AX using a Laccase/TEMPO and a TEMPO/BAIB system, respectively, to improve the functional properties of the native AX. Both studies observed the preferred conversion of Ara*f* to the aldehyde form rather than the uronic acid form. Therefore, attention must be paid to oxidized products other than uronic acids when TEMPO-oxidizing polysaccharides. Additionally, Bowman, Dien, O'Bryan, Sarath, and Cotta (2011) oxidized AX from birch, wheat and switchgrass (SG) using a 4-Acetamido-TEMPO/NaOCl/NaBr system to distinguish the isomers Ara and Xyl, by selectively oxidizing Ara*f* to AraA*f*. These authors observed an increment of 14 Da in oxidized-oligosaccharides comparatively to non-oxidized ones in hydrophilic interaction liquid chromatography (HILIC-LC)-MS analysis of the partially-acid depolymerized oxidized SG AX, proving the presence of AraA*f* as an oxidized product derived from Ara*f*. However, this study did not indicate whether the native AX structure was kept after oxidation, by solely converting the Ara side chains into an AraA residue, or even arabinose removal, degradation or formation of side oxidation products.

Our study aims to investigate if TEMPO-oxidation of an AX will selectively oxidize the Ara*f* side chains to AraA*f* without major changes in the native AX structure, allowing us to obtain a polyuronide with a substitution pattern closely related to its parental arabinoxylan. For this, TEMPO/$NaClO_2$/NaOCl system at pH 4.6, with various TEMPO:$NaClO_2$:NaOCl ratios, was selected to oxidize an AX. The TEMPO oxidized-AX structure was characterized in terms of molecular weight distribution, sugar and linkage composition, and identification of oxidized compounds by NMR spectroscopy.

2. Materials and methods

2.1. Materials

The polysaccharide substrate used to perform the TEMPO-mediated oxidation was a commercial wheat arabinoxylan (AX) of medium viscosity (Ara:Xyl = 38:62, Purity > 95 %, Megazyme, Wicklow, Ireland). L-(+)-Arabinose (Ara) (99 %), Maleic acid (98 %), sodium borodeuteride (NaBD, 98 %, 41.86 g/mol), trifluoroacetic acid (TFA, 99 %), HCl in dried methanol (3 M), deuterium oxide (D_2O, 99.9 %), and sodium nitrate ($NaNO_3$, > 99 %, 84.99 g/mol) were purchased from Sigma-Aldrich (St. Louis, MO, USA). D-(+)-Xylose (Xyl) (> 99 %), 2,2,6,6-tetramethylpiperidine-1-oxyl radical (TEMPO, 98 %, 156.25 g/mol), $NaClO_2$ (80 %, 90.44 g/mol), sodium hypochlorite solution (6–14 % active chlorine NaOCl), N-Cyclo-N'-[2-(N-methylmorpholino)-ethyl]-carbodiimide 4-toluolsulfonate, and sodium acetate (NaOAc) anhydrous were purchased from Merck (Darmstadt, Germany). Methyl iodide (CH_3I) was obtained from VWR (Rue Carnot, France), lithium aluminum deuteride ($LiAlD_4$, > 98 %, 41.99 g/mol) was obtained from BOC Sciences (NY, USA), and acetonitrile from Biosolve (Valkenswaard, The Netherlands). All water was purified in a Milli-Q system from Millipore (Molsheim, France), unless otherwise mentioned.

2.2. Oxidation of arabinoxylan

Various TEMPO-oxidation systems were preliminarily screened to oxidize AX, namely TEMPO/$NaClO_2$/NaOCl and TEMPO/NaOCl systems at pH 4.6 (24 h at 35 °C) (Saito et al., 2010; Tamura et al., 2010; Tanaka et al., 2012), and TEMPO/BAIB (1:9 mol equivalent of Ara) and TEMPO/BAIB/NaOCl (1:9:1.5 mol equivalent of Ara) in Acetonitrile: Water (3:1, v/v) for 2 h at 0 °C followed by 4 h at room temperature (RT) (Börjesson & Westman, 2016; Tojo & Fernández, 2007). TEMPO/$NaClO_2$/NaOCl and TEMPO/NaOCl systems were also tested in Acetonitrile:Water (3:1, v/v) and at pH 4.6 for 2 h at 0 °C followed by 4 h at RT. TEMPO/$NaClO_2$/NaOCl system at pH 4.6 for 24 h at 35 °C using a TEMPO/$NaClO_2$/NaOCl ratio of 0.2:2.6:0.4 (per mol equivalent of Ara) was the system that gave more promising results. Based on this, TEMPO/$NaClO_2$/NaOCl oxidation of AX was selected to be further investigated in this study by testing various TEMPO/$NaClO_2$/NaOCl ratios (Table 1). TEMPO and NaOCl were tested in two levels, 0.2 and 1.0, and 0.4 and 1.5 mol equivalent of Ara, respectively, and $NaClO_2$ was kept constant (Table 1).

Oxidation of the wheat AX was done using the TEMPO/$NaClO_2$/NaOCl system at pH 4.6 using a protocol adapted from Tamura et al. (2010). TEMPO/$NaClO_2$/NaOCl mixtures were tested in three different mol ratios per mol of primary OH group (C5-OH of Ara) (Table 1). 200 mg of AX in a final reaction volume of 40 mL, comprising 0.2 M NaOAc buffer pH 4.6, and TEMPO, $NaClO_2$ and NaOCl solutions as listed in Table 1 was used to perform the reaction.

AX powder was completely solubilized in 0.2 M NaOAc buffer at pH 4.6 (different volumes of buffer were added depending on the oxidation condition described in Table 1) under magnetic stirring in a glass flask. Stock solutions of TEMPO and $NaClO_2$ were prepared in 0.2 M NaOAc buffer to a final concentration of 0.05 mmol/mL and 0.40 mmol/mL, respectively. The required volume of 0.05 mmol/mL TEMPO and 0.40 mmol/mL $NaClO_2$ to reach the desired concentration in the final reaction volume (Table 1) were mixed and incubated under magnetic stirring for 10 min at RT. Thereafter, the pre-incubated TEMPO/$NaClO_2$ solution was added to the flask containing the AX solution in buffer. Then, variable volumes of 6–14 % NaOCl solution to be added to each

Table 1
Sample identification and reaction conditions used to TEMPO-oxidize arabinoxylans. Reactions were performed in 0.2 M NaOAc buffer pH 4.6 for 24 h at 35 °C with variable molar ratios of TEMPO:$NaClO_2$:NaOCl. Final concentrations of AX in mg/mL, and TEMPO, $NaClO_2$, and NaOCl in mM used during oxidation reaction are mentioned. Values within parentheses correspond to the TEMPO:$NaClO_2$:NaOCl ratio per mol of C5-OH.

Sample name[a]	C_{AX} (mg/mL)	C_{TEMPO} (mM)	C_{NaClO2} (mM)	C_{NaOCl} (mM)
ox-$AX^{1.0:2.6:1.5}$	5.0	14 (1.0)	38 (2.6)	22 (1.5)
ox-$AX^{0.2:2.6:1.5}$	5.0	3 (0.2)	38 (2.6)	22 (1.5)
ox-$AX^{1.0:2.6:0.4}$	5.0	14 (1.0)	38 (2.6)	6 (0.4)

[a]- ox-AX^{b} refers to the oxidized wheat arabinoxylan (ox-AX) obtained with a [b] TEMPO:$NaClO_2$:NaOCl ratio per mol of C5-OH.

oxidation condition to have the desired final NaOCl concentration was added at once to the flask to start the reaction. The flask was closed, and the reaction was carried out in an incubator for 24 h at 35 °C under shaking (100 rpm). The reaction was quenched by adding cold ethanol (96 % v/v) to a final concentration of 70 % (v/v) to the solution, followed by stirring for 1 h at RT. The precipitate formed containing the oxidized (ox-) AX was recovered by centrifugation (11 571*g*, 15 °C, 30 min), washed with 70 % (v/v) EtOH by stirring for 1 h at RT, and collected by centrifugation as mentioned above. Afterwards, the ox-AX was re-suspended in demi-water, dialyzed (cut-off 12−14 kDa, Medicell Membranes Ltd, London, UK) against demi-water, and freeze-dried to obtain homogeneous dried material, yielding the final ox-AX samples. Native AX and ox-AX samples were further characterized.

2.3. Molecular weight distribution of polysaccharides

The molecular weight (Mw) was determined by high performance size exclusion chromatography (HPSEC). HPSEC analysis was carried out on an Ultimate 3000 system (Dionex, Sunnyvale, CA, USA) coupled to a Shodex RI-101 detector (Showa Denko K.K., Tokyo, Japan). The system was equipped with a set of three TSK-Gel Super columns 4000AW, 3000AW, and 2500AW (6 mm ID ×150 mm per column, 6 μm) connected in series preceded by a TSK Super AW-L guard column (4.6 mm ID ×35 mm, 7 μm), all from Tosoh Bioscience (Tokyo, Japan). The column oven temperature was maintained at 55 °C during analysis. Standards and samples were dissolved in water to a concentration of 1.0 mg/mL. 10 μL of sample was injected onto the system and eluted with 0.2 M $NaNO_3$ solution at a flow rate of 0.6 mL/min. Although the final oxidized products are negatively charged, calibration of the SEC columns was done with pullulan standards (0.180–708 kDa; Polymer Laboratories, Church Stretton, UK) since the parental AX is neutral and ox-AX moderately charged. Calibrating the columns with available pectin standards would provide incorrect Mw values for the AX and also not give accurate results for ox-AX either, as pectins might be heavily charged. The retention times of the monodisperse pullulan standards were used to obtain the calibration curve to determine the apparent Mw of the samples. The collected data was analysed using Chromeleon 7.2 software (Dionex Corporation).

2.4. Monosaccharide composition analysis by HPAEC-PAD

(ox-)AX samples were methanolysed using 2.0 M HCl in dried methanol for 16 h at 80 °C, and the released methyl-glycosides were converted to their non-methylated form via TFA acid hydrolysis in accordance with De Ruiter, Schols, Voragen, and Rombouts (1992) and ter Haar et al. (2010). Hydrolysates were diluted with water to about 25 μg/mL and the sugars released were analysed by High-Performance Anion-Exchange Chromatography with Pulsed Amperometric Detection (HPAEC-PAD). An ICS-5000 HPLC system (Dionex, Sunnyvale, CA, USA) equipped with a CarboPac PA1 guard column (2 mm ID ×50 mm) and a CarboPac PA-1 column (2 mm ID ×250 mm; both from Dionex) was used for this analysis. Detection of the eluted compounds was performed by an ED40 EC-detector running in the PAD mode (Dionex). 10 μL of the diluted hydrolysate was injected on the system. Mobile phases used to elute the compounds were kept under helium flushing and the column temperature was 20 °C. A flow rate of 0.4 mL/min was used with the following gradient of 0.1 M sodium hydroxide (NaOH: A) and 1.0 M NaOAc in 0.1 M NaOH (B): 0−35 min, 100 % milli-Q water; 35.1 min, 100 % A; 35.2−50 min, 0–40 % B; 50.1−55 min, 100 % B; 55.1–63.0 min, 100 % A; 63.1–78.0 min, 100 % milli-Q water. A post-column alkali addition (0.5 M NaOH; 0.1 mL/min) was used from 0.0 to 34.9 min and from 68.1 to 78.0 min. All samples were analysed in duplicate. Standards of Ara and Xyl in a concentration range of 1.0−150 μg/mL were used for quantification. The collected data was analysed using Chromeleon 7.2 software (Dionex Corporation).

2.5. Purification of oxidized compounds from the ox-AX$^{1.0:2.6:0.4}$ hydrolysate by SPE

To isolate the oxidized compounds present in the ox-AX$^{1.0:2.6:0.4}$ hydrolysate (Section 2.4), the sample was fractionated using solid phase extraction (SPE) as described by Sun et al. (2020) with some modifications. About 100 μg of hydrolysate was dissolved in water and loaded onto a Supelclean™ ENVI-Carb™ column (3.0 mL, Sigma-Aldrich), which was activated with 1.5 mL acetonitrile:water (80:20; v/v) containing 0.1 % (v/v) TFA, and water (3 × 1.5 mL). Neutral monosaccharides were eluted from the column with water (4 × 1.5 mL), whereas retained oxidized compounds were eluted with three times 1.5 mL of acetonitrile:water (60:40; v/v) containing 0.05 % (v/v) TFA. Water and acetonitrile:water:TFA fractions were dried under a stream of nitrogen at RT, yielding the fractions Hydr_ox-AX$^{1.0:2.6:0.4}$_H_2O and Hydr_ox-AX$^{1.0:2.6:0.4}$_TFA, respectively. Fractions were analysed by ^{1}H-NMR (Section 2.6) and Hydr_ox-AX$^{1.0:2.6:0.4}$_TFA was further analysed by 2D-NMR COSY (Section 2.6).

2.6. Analysis by ^{1}H-NMR and ^{1}H-^{1}H COSY

Dried hydrolysates of the native AX and ox-AX$^{1.0:2.6:0.4}$ samples, and the Hydr_ox-AX$^{1.0:2.6:0.4}$_H_2O and Hydr_ox-AX$^{1.0:2.6:0.4}$_TFA fractions collected from SPE were re-suspended in D_2O and freeze-dried to exchange the free —OH groups by -OD. Samples were subsequently dissolved in D_2O to approximately 0.2 mg/mL containing 0.2 mg/mL maleic acid (internal standard, IS). Additionally, dried AX and ox-AX$^{1.0:2.6:0.4}$ samples were dissolved in D_2O to approximately 3.7 mg/mL containing 0.2 mg/mL IS. All samples were analysed by ^{1}H-NMR and the Hydr_ox-AX$^{1.0:2.6:0.4}$_TFA fraction was further analysed by homonuclear ^{1}H-^{1}H correlation (COSY) to identify AraA and assign ^{1}H-NMR signals. Both ^{1}H-NMR and COSY-NMR experiments were carried out on a 600 MHz (14.1 T) Bruker Avance III NMR spectrometer (Bruker BioSpin, Switzerland) equipped with a 5-mm cryo-probe at 298 K. The 1D ^{1}H-NMR spectra were recorded with a noesygppr1d pulse sequence. The size of the FID was 65k. In total, 256−512 scans were collected with a relaxation time of 1 s and an acquisition time of 4 s. Low power water suppression (16 Hz) was applied for 0.1 s. The 90° pulse length (~7.6 μs) and receiver gain were determined automatically. The data was processed with Bruker TopSpin 4.0.7 software. Fourier transformation with exponential window function and a line broadening factor of 0.3 Hz were applied, followed by automatic phase- and baseline correction. The 2D ^{1}H-^{1}H COSY experiments were recorded with a cosygpprqf pulse sequence. The spectral widths were 4 ppm in both dimensions, with the O1 at 4.7 ppm to centre around the aromatic region. The number of scans was 128 with 16 dummy scans. 256 increments were collected in F1, and 1024 increments in F2. The recycle delay was 2 s.

A relative monosaccharide quantification for AX and ox-AX$^{1.0:2.6:0.4}$ was performed based on the sum of the ^{1}H-NMR signal integrals derived from each identified sugar (I_{sugar} (Eq. (1)) (Malz & Jancke, 2005; Merkx et al., 2018).

$$Sugar\ (\%) = \frac{I_{Sugar}}{\sum(I_{Ara} + I_{Xyl} + I_{AraA})} \quad (1)$$

I_{sugar} corresponds to either Ara (I_{Ara}), Xyl (I_{Xyl}), or AraA (I_{AraA}) and is the sum of the α- and β-signal integrals of the anomeric proton of Ara, Xyl and AraA, respectively.

2.7. Glycosidic linkage and substitution analysis

Carboxyl groups of the uronic acids present in the ox-AX$^{1.0:2.6:0.4}$ sample were reduced to neutral monosaccharides using two different methods. The uronic acids present on the polysaccharide were twice reduced with Carbodiimide/$NaBD_4$ prior to linkage analysis in accordance with Taylor and Conrad (1972), or alternatively were reduced

with $LiAlD_4$ upon per-methylation of the polysaccharide as described by Pandeirada et al. (2019). Carboxyl-reduced and non-reduced ox-$AX^{1.0:2.6:0.4}$, and AX samples were subjected to per-methylation analysis to access the glycosidic linkage patterns. Per-methylation was performed with a modification to the method described by Nunes et al. (2012) and Pandeirada et al. (2019), by replacing the argon atmosphere by nitrogen. Partially methylated polysaccharide samples were converted into their partially methylated alditol acetate (PMAA) forms by hydrolysis, reduction and acetylation (Pandeirada et al., 2019), and then analysed by gas chromatography coupled to mass spectrometry (GC–MS). PMAA samples were analysed using a GC (Trace GC Ultra™, Thermo Scientific) with a split injector equipped with a 30 m DB 35MS column (Restek, Bellefonte, PA, USA) with diameter and film thickness of 0.25 mm and 0.25 μm, respectively, and connected to a Dual Stage Quadrupole (DSQII, Thermo Scientific) mass selective detector. 1.0 μL of sample was injected in the PTV split mode with the injector operating at an initial temperature of 190 °C, ramped to 275 °C at 14.5 °C/min, holding for 1.0 min. The GC oven temperature program was set to an initial temperature of 120 °C, raised to 250 °C at 2.5 °C/min, holding for 5 min. The pressure of the carrier gas (He) was set at 100 kPa. The mass spectrometer was operated in the electron impact mode (EI) at 70 eV scanning the range 50–450 *m/z*, in full scan acquisition mode. The collected data was analysed using Xcalibur 4.1 software (Thermo Scientific) and chromatographic peaks were identified comparing all mass spectra with a laboratory made database of PMAAs. As reduction of the ox-$AX^{1.0:2.6:0.4}$ sample with carbodiimide/$NaBD_4$ prior to per-methylation gave more reliable results, only these results will be shown.

3. Results and discussion

In this study, oxidation of arabinoxylan (AX) using a TEMPO/$NaClO_2$/NaOCl system at pH 4.6 was performed to investigate if the TEMPO-oxidation will selectively oxidize the Ara*f* side chains of an AX to arabinuronic acid (AraA*f*), allowing us to yield a polyuronide type structure (arabinuronoxylan) with a structure resembling the parental AX structure. A preliminary oxidation study on wheat AX indicated that a TEMPO/$NaClO_2$/NaOCl oxidation system using a ratio of 0.2:2.6:0.4 (per mol equivalent of Ara) gave preferential results with an oxidized-AX with an apparent molecular weight (Mw) identical to the native AX (Fig. S1) and a degree of Ara oxidation of about 54 (w/w) % (Table S1), based on the Ara content decrease. Consequently, TEMPO and NaOCl were tested in variable ratios and in higher amounts, 1.0 and 1.5 mol equivalent of Ara (Table 1), respectively, when compared to the preliminary condition to ensure that all available primary OH groups would be oxidized to aldehydes and further oxidized to carboxylic groups by NaO_2Cl. NaO_2Cl was kept constant, as it was being used in an amount that should ensure full conversion of aldehydes to carboxyl groups during reaction, as it is the primary oxidant (Brückner, 2010; Isogai et al., 2018; Tojo & Fernández, 2007). From these AX oxidations with variable TEMPO:$NaClO_2$:NaOCl ratios per mol of primary hydroxyl group of Ara (C5-OH), three oxidized (ox-)AX samples, ox-$AX^{1.0:2.6:1.5}$, ox-$AX^{0.2:2.6:1.5}$, and ox-$AX^{1.0:2.6:0.4}$ were obtained.

3.1. Molecular weight distribution of TEMPO oxidized AX samples

To monitor if the TEMPO-oxidation reaction would lead to AX degradation, the Mw distribution of the native and ox-AX samples was analysed by HPSEC (Fig. 1). The apparent Mw of wheat AX was determined by using the retention time of the maximum value of the peak, which gave a Mw value for AX of around 400 kDa, in accordance with previous reports (200−700 kDa) (Dervilly, Saulnier, Roger, & Thibault, 2000; Dervilly-Pinel, Thibault, & Saulnier, 2001; Izydorczyk, 2009; Saulnier, Sado, Branlard, Charmet, & Guillon, 2007). Compared to AX, the apparent Mw of the three ox-AX samples decreased and it was noted that the ox-AX samples were more polydisperse, as observed by the broad peaks in Fig. 1. This can be due to the charge effect due to polymer oxidation, or due to polymer degradation. Furthermore, compared to the preliminary ox-$AX^{0.2:2.6:0.4}$, whose apparent Mw was similar to the Mw of the native AX (Fig. S1A), these results suggest that increasing the amount of TEMPO and/or NaOCl (from 0.2 to 1.0, and from 0.4 to 1.5 mol eq. of C5-OH, respectively, Table 1) might favor polymer degradation. The smallest decrease in the apparent Mw was obtained for ox-$AX^{1.0:2.6:0.4}$ (175 kDa), followed by ox-$AX^{0.2:2.6:1.5}$ (124 kDa) and ox-$AX^{1.0:2.6:1.5}$ (106 kDa). These results indicate that, within the conditions tested in our work, NaOCl used at 1.5 mol equivalent of C5-OH potentiates polymer degradation, especially when TEMPO was only present at low level. This suggests that TEMPO can protect against polymer degradation, as reported before (Spier et al., 2017). Furthermore, the polymer degradation likely boosted by an elevated amount of NaOCl is probably be due to non-selective oxidation of vicinal secondary hydroxyl groups at C-2 and/or C-3 of Ara and/or Xyl to carbonyl groups triggered by NaOCl (Rejzek, Mukhopadhyay, Wenzel, Lam, & Field, 2007), which probably caused instability and degradation of the xylan

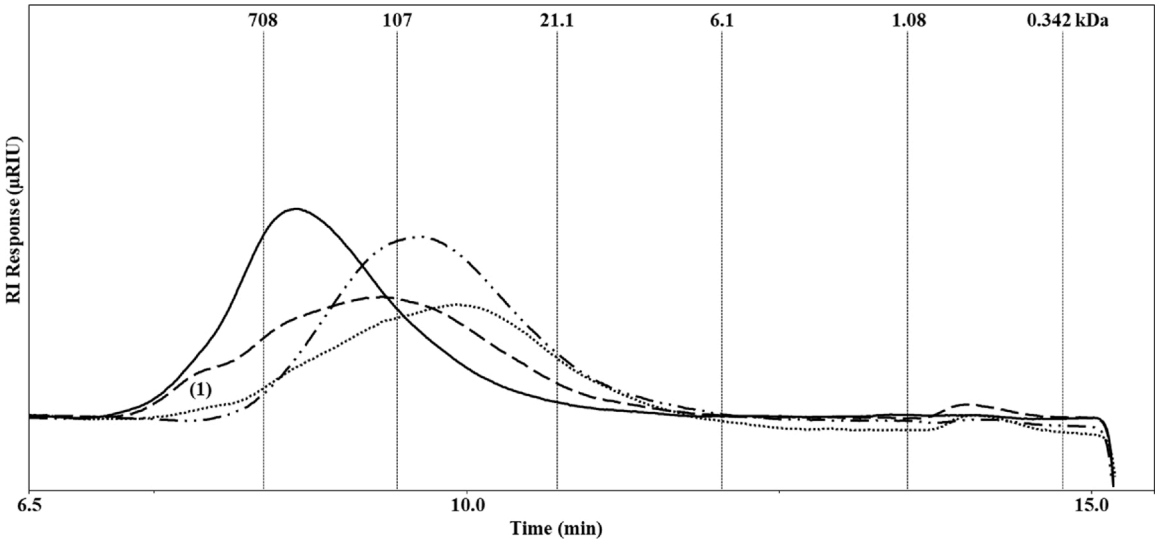

Fig. 1. HPSEC elution patterns of the native AX (—), and of the TEMPO oxidized AX samples ox-$AX^{1.0:2.6:1.5}$ (·····), ox-$AX^{0.2:2.6:1.5}$ (-·-·-·-), and ox-$AX^{1.0:2.6:0.4}$ (- - - -). Pullulan standards were used to calibrate the system. Population (1) present in ox-$AX^{1.0:2.6:1.5}$ and ox-$AX^{1.0:2.6:0.4}$.

backbone. Despite the decrease in the Mw, the still high Mw of the ox-AX samples indicates that the AX native structure could be largely conserved. This result agrees with literature suggesting that a TEMPO/$NaClO_2$/NaOCl approach only leads to minimal polysaccharide depolymerization (Saito et al., 2010; Tamura et al., 2009, 2010; Tanaka et al., 2012).

Interestingly, within the ox-AX samples, the oxidized samples obtained with the highest amount of TEMPO (ox-$AX^{1.0:2.6:1.5}$ and ox-$AX^{1.0:2.6:0.4}$) displayed a second population being more shifted to the left in the HPSEC elution pattern (population (1) in Fig. 1). This population has an apparent Mw higher than 400 kDa and is especially present when higher amounts of TEMPO and lower amounts of NaOCl were used (ox-$AX^{1.0:2.6:0.4}$, Fig. 1). The presence of this population suggests that part of the ox-$AX^{1.0:2.6:0.4}$ molecules have an increased hydrodynamic volume, probably due to an increase in repulsing anionic groups on the polymer formed during TEMPO oxidation (Guo, Ai, & Cui, 2018). This phenomenon was seen before by ter Haar et al. (2010) studying TEMPO/-NaBr/NaOCl oxidized starches with different degrees of oxidation (DO). Thus all together, it can be speculated that among the various ox-AX samples, ox-$AX^{1.0:2.6:0.4}$ is the most oxidized AX, followed by ox-$AX^{1.0:2.6:1.5}$ and ox-$AX^{0.2:2.6:1.5}$. Moreover, this suggests that TEMPO is key in the oxidation reaction, and that increasing the NaOCl does not lead to an increase in the oxidation level but preferably boosts polymer degradation. Although working at a different pH, this agrees with the findings that in alkaline medium, NaOCl can lead to more depolymerization (Lin et al., 2019; Shibata & Isogai, 2003), while it also has been reported that increasing the NaOCl in a TEMPO:NaBr:NaOCl system at alkaline pH leads to a higher content in carboxyl groups (Huang et al., 2013; Lin et al., 2019).

3.2. Sugar composition of TEMPO-oxidized AX samples

The sugar composition of the native and TEMPO ox-AX samples is shown in Table 2. AX was composed of Xyl (58.9 %, w/w) and Ara (31.6 %, w/w) with a molar Ara:Xyl ratio of approximately 0.5, which is in accordance with literature for wheat AX (Gruppen, Hamer, & Voragen, 1992; Izydorczyk & Biliaderis, 1993; Izydorczyk, 2009; Saulnier et al., 2007). Regarding the ox-AX samples, ox-$AX^{1.0:2.6:1.5}$ was composed of 57.5 % (w/w) Xyl, and both ox-$AX^{0.2:2.6:1.5}$ and ox-$AX^{1.0:2.6:0.4}$ were composed of 53.9 % (w/w) Xyl (Table 2). This showed that Xyl was largely recovered (> 80 %) in all ox-AX samples. The high recovery of Xyl indicates that none or minor changes of the xylan backbone have occurred during TEMPO oxidation, as expected, since TEMPO preferable oxidizes primary alcohols with minimal effect on secondary alcohols, as those present in Xyl*p* units (Bowman et al., 2011; Davis & Flitsch, 1993; Takeda, Miller, & Fry, 2008).

Contrarily, the Ara content in the ox-AX samples abruptly decreased comparatively to the parental AX sample (31.6 %, w/w). ox-$AX^{1.0:2.6:1.5}$, ox-$AX^{0.2:2.6:1.5}$ and ox-$AX^{1.0:2.6:0.4}$ were respectively composed of 0.9 %, 9.5 % and 2.1 % (w/w) of Ara (Table 2), explaining the very low recovery yield of Ara (approximately 3 %, 30 % and 6 % for ox-$AX^{1.0:2.6:1.5}$, ox-$AX^{0.2:2.6:1.5}$ and ox-$AX^{1.0:2.6:0.4}$, respectively). This shows that Ara was preferentially TEMPO-oxidized, as expected since only the primary alcohols of Ara units are susceptible to oxidation (Bowman et al., 2011; Saito et al., 2010; Spier et al., 2017; Tojo & Fernández, 2007). The large decrease in Ara suggests a degree of Ara oxidation higher than 90 % for ox-$AX^{1.0:2.6:1.5}$ and ox-$AX^{1.0:2.6:0.4}$, and 70 % for ox-$AX^{0.2:2.6:1.5}$. These values agree with HPSEC results suggesting that ox-$AX^{1.0:2.6:0.4}$ and ox-$AX^{1.0:2.6:1.5}$ had the highest DO, followed by ox-$AX^{0.2:2.6:1.5}$. Connected to the decrease in Ara*f*, a new compound (coded ox-Product in Table 2) was detected in the HPAEC elution pattern of the ox-AX hydrolysates (Supplementary Material, Fig. S2). This novel compound, which eluted at retention times commonly found for uronic acids (results not shown), might be derived from the oxidation of Ara into its uronic acid form (arabinuronic acid, AraA). Due to the lack of standards, the identification and quantification of this new compound as Ara*f* could not be ascertained by HPAEC. Accordingly, the sugar recovery was calculated for all ox-AX samples considering only Ara and Xyl, which led to an expected low sugar recovery ranging from 50.1 to 62.1 % (w/w) (Table 2).

3.3. Characterization of ox-$AX^{1.0:2.6:0.4}$ by 1D- and 2D-NMR

Together, the sugar composition and the Mw distribution of the ox-AX samples suggested that ox-$AX^{1.0:2.6:0.4}$ had the highest DO of Ara and was least degraded. Therefore, this sample was chosen to be further characterized to elucidate the structure of the ox-product recognised by HPAEC. The ^{1}H-NMR spectra of the anomeric region of the monosaccharides present in the hydrolysates of the AX and ox-$AX^{1.0:2.6:0.4}$ samples are shown in Fig. 2. Full ^{1}H-NMR spectra and signal integrals are shown in supplementary material (Fig. S3). For AX hydrolysate (Fig. 2, line A), the doublets at δ 5.15 ppm and δ 4.48 ppm correspond to the α-anomeric proton derived from Xyl and Ara, respectively, whereas the doublets at δ 4.53 ppm and δ 5.20 ppm are derived from the β-anomeric proton of Xyl and Ara, respectively, according to Benesi, Falzone, Banerjee, and Farber (1994).

The α/β-anomeric proton signal intensities derived from Xyl in the ^{1}H-NMR spectrum of both AX and ox-$AX^{1.0:2.6:0.4}$ hydrolysates (Fig. 2, line A and B, respectively) were comparable. Contrarily, the α/β-anomeric proton signal intensities derived from Ara largely decreased in the ox-$AX^{1.0:2.6:0.4}$ hydrolysate (Fig. 2, line B) relatively to the ones derived from AX (Fig. 2, line A). These observations agree with the results obtained by HPAEC. Additionally, the ^{1}H-NMR spectrum of the ox-$AX^{1.0:2.6:0.4}$ hydrolysate exhibited three new doublets, one at around δ 4.60 ppm (peak c, Fig. 2, line B) and two between δ 5.3–5.4 ppm (peaks b and a, Fig. 2, line B), in comparison to AX hydrolysate. Considering that TEMPO oxidizes Ara to AraA, the doublets of the α/β-anomeric protons of AraA should be less protected than the respective doublets of Ara, due to the presence of a carboxyl group in the AraA structure, as observed for e.g. GalA comparatively to Gal (Kiemle, Stipanovic, & Mayo, 2004; Merkx et al., 2018). Thus, two out of the three new observed doublets that appear in the anomeric region in Fig. 2

Table 2
Yields, sugar composition and recovery of the native AX, and of the oxidized AX (ox-AX) samples using various ratios of TEMPO:$NaClO_2$:NaOCl.

Sample	Yield[a] (%, w/w)	Carbohydrate composition (%, w/w)[b]				Sugar Recovery (%, w/w)[c]
		Ara	Xyl	Total	Ox-Product	
AX	–	31.6 ± 0.1	58.9 ± 0.5	90.5 ± 0.6	–	–
ox-$AX^{1.0:2.6:1.5}$	97	0.9 ± 0.0	56.5 ± 0.6	57.5 ± 0.6	+	55.7 ± 0.6
ox-$AX^{0.2:2.6:1.5}$	98	9.5 ± 0.2	53.9 ± 0.4	63.4 ± 0.6	+	62.1 ± 0.6
ox-$AX^{1.0:2.6:0.4}$	91	2.1 ± 0.1	53.9 ± 1.9	55.9 ± 1.9	+	50.1 ± 1.8

ox-AX^{b}: oxidized arabinoxylan (ox-AX) obtained with a [b] TEMPO:$NaClO_2$:NaOCl ratio per mol of C5-OH of Ara.

[a] Yield in weight % relative to the native AX.

[b] Results are expressed as average (n = 2) weight % of sample. Presence of the oxidized product formed during TEMPO-oxidation reaction is indicated with +, and absence with –.

[c] Results are expressed as average (n = 2) weight % of native AX. ox-Product is not accounted in the sugar recovery of ox-AX samples.

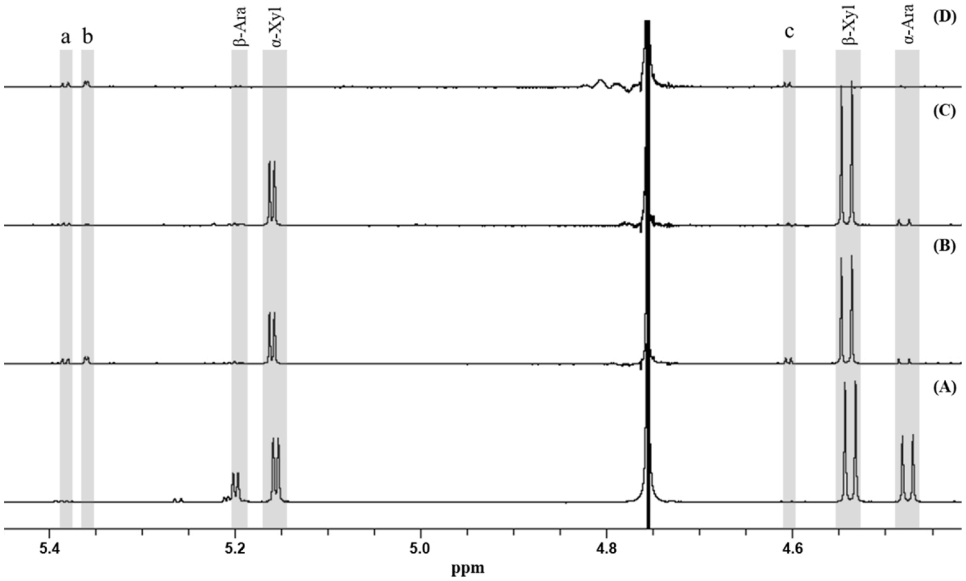

Fig. 2. ^{1}H-NMR spectra (600 MHz) of the anomeric region of the monosaccharides present in the hydrolysates of the native AX (**A**), and ox-AX$^{1.0:2.6:0.4}$ (**B**), and of the fractions Hydr_ox-AX$^{1.0:2.6:0.4}$_H_2O (**C**) and Hydr_ox-AX$^{1.0:2.6:0.4}$_TFA (**D**) obtained from SPE of the hydrolysate of the ox-AX$^{1.0:2.6:0.4}$ sample with water and acetonitrile:water (60:40; v/v) containing 0.05 % (v/v) TFA, respectively. α- and β-anomeric proton signals of Xyl and Ara, and additional chemical shifts arising in the anomeric region (a, b, and c) of the ox-AX$^{1.0:2.6:0.4}$ sample compared to the native AX are highlighted in grey boxes.

(signals a, b, and c) might be derived from the H-1 of α/β-AraA.

To assign the new doublets that appear in the anomeric region of the ^{1}H-NMR spectrum (signals a, b, and c in Fig. 2, line B) of the ox-AX$^{1.0:2.6:0.4}$ hydrolysate to their corresponding protons and to unveil the structure of the ox-product present in this sample, the ox-AX$^{1.0:2.6:0.4}$ hydrolysate was fractionated by SPE. This yielded a neutral Hydr_ox-AX$^{1.0:2.6:0.4}$_H_2O fraction retaining the Ara and Xyl residues (still) present (Fig. 2, line C), and an acidic Hydr_ox-AX$^{1.0:2.6:0.4}$_TFA fraction containing the ox-product (Fig. 2, line D). Consequently, this fraction was further analysed by homonuclear ^{1}H-^{1}H correlation (COSY) (Fig. 3) to reveal the structure of the ox-product.

The 2D ^{1}H-^{1}H COSY spectrum enabled identification of the α- and β-conformations of the H-1, H-2, H-3, and H-4 signals of AraA (Fig. 3 and Table 3), which appeared from the least to the most shielded chemical

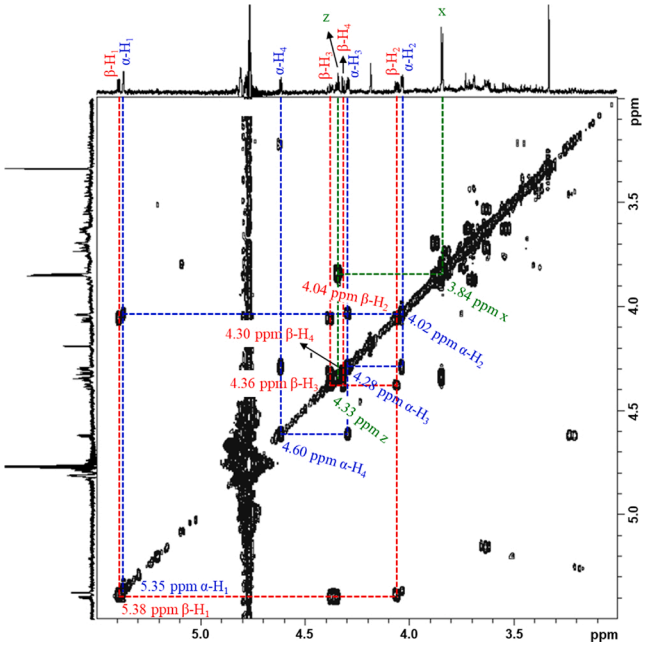

Fig. 3. The 2D ^{1}H-^{1}H COSY spectrum of the Hydr_ox-AX$^{1.0:2.6:0.4}$_TFA fraction in D_2O. Signal assignments of the α- and β-conformation protons of AraA*f* are shown in blue and red, respectively. Signal at δ 4.8 ppm and at δ 3.33 ppm are due to residual H_2O and methanol, respectively.

shift signal as follows: β-H1 (5.38 ppm) > α-H1 > α-H4 > β-H3 > β-H4 > α-H3 > β-H2 > α-H2 (4.02 ppm). This chemical shift sequence and the ^{1}H-^{1}H coupling constants obtained in our study for AraA (Table 3) are similar to the ones observed by Wu and Serianni (1991), who oxidized Ara to AraA via methyl glycosidation of Ara, followed by oxidation of methyl-Ara*f* to methyl-AraA*f* using platinum oxide, and hydrolysis of the methyl-AraA*f* to AraA*f* before analysis by ^{1}H-NMR spectroscopy. These authors verified that the H-1 of the α- and β-conformation of AraA were only δ 0.03 ppm separated from each other, which was also seen in our work (δ β-H1 - δ α-H1 = δ 0.03 ppm). The 2D-NMR results proved that part of the Ara was selectively oxidized to AraA, resulting in an anionic polymer (arabinuronoxylan), which has potential to be further explored for its polyuronides properties (Pierre et al., 2017). Additionally, 2D-NMR also allowed us to unveil the three new doublets that appeared in the ^{1}H-NMR spectrum of the ox-AX$^{1.0:2.6:0.4}$ hydrolysate. The doublets at δ 5.38 ppm and δ 5.35 ppm (signal a and b, respectively, Fig. 2, lines B and D) are the H-1 signals of the β-AraA and α-AraA, respectively, whereas the doublet at δ 4.6 ppm (signal c, Fig. 2, lines B and D) is the H-4 signal of the α-AraA. Considering only the anomeric signal integrals (Supplementary Material, Fig. S3) derived from the α/β-forms of AraA, Ara, and Xyl in the ^{1}H-NMR spectrum, the relative content of AraA in the ox-AX$^{1.0:2.6:0.4}$ sample was approximately 7 % (mol/mol), with 4 % and 89 % (mol/mol) accounting for Ara and Xyl, respectively. This relative AraA content is rather low when compared to the Ara content (35 %, mol/mol). Consequently, from these results, some AX debranching cannot be ruled out during TEMPO-oxidation.

Apart from AraA chemical shifts, other signals were seen in the 2D-NMR spectrum of the Hydr_ox-AX$^{1.0:2.6:0.4}$_TFA fraction. The doublet at δ 3.84 ppm (X in Fig. 3 and Table 3) and the triplet at δ 4.33 ppm (Z in Fig. 3 and Table 3) had vicinal coupling ($^{3}J_{HH}$ of 4.1 Hz). As the chemical shift at δ 4.33 ppm (Z) is a triplet, it must have two coupling partner protons, meaning that the doublet at δ 3.84 ppm (X) must be composed of two proton nuclei, which couple identically with proton Z. This would explain the double signal intensity obtained for the doublet X in comparison to the triplet Z (Supplementary Material, Fig. S3), since the signal integral is proportional to the number of nuclei contributing to the signal (Malz & Jancke, 2005). Hence, the compound comprising the X and Z signals was putatively assigned to arabinaric acid (Table 3), the aldaric acid form of arabinose (arabinaric acid structure is shown in Supplementary Material, Fig. S3), which can explain the relatively low AraA level in the ox-AX$^{1.0:2.6:0.4}$ hydrolysate. Besides X and Z signals, other chemical shifts were seen in the 2D-NMR spectrum of the Hydr_ox-AX$^{1.0:2.6:0.4}$_TFA fraction (singlet at δ 4.18 ppm; signals

Table 3
^{1}H chemical shifts (ppm) of the protons assigned to α- and β-AraA by 2D ^{1}H-^{1}H COSY, values of the $^{3}J_{HH}$ coupling constant of these protons in Hz, and type of signal of each proton.

Compound	Chemical Shift (ppm)	Proton	$^{3}J_{HH}$ Coupled nuclei	$^{3}J_{HH}$ Coupling constant (Hz)	Type of signal
α-D-Arabinuronic acid	5.35	H1	H1-H2	1.8	Doublet
	4.02	H2	H2-H1	1.8	Double doublet
			H2-H3	2.9	
	4.28	H3	H3-H2	2.9	Double doublet
			H3-H4	4.1	
	4.6	H4	H4-H3	4.1	Doublet
β-D-Arabinuronic acid	5.38	H1	H1-H2	4.3	Doublet
	4.04	H2	H2-H1	4.3	Double doublet
			H2-H3	6.4	
	4.36	H3	H3-H2	6.5	Double doublet
			H3-H4	5.7	
	4.30	H4	H4-H3	5.7	Doublet
Tentative compound assigned to δ 3.84 ppm and δ 4.33 ppm					
Arabinaric acid	3.84	X (H2, H4)	H2-H3 H4-H3	4.1	Doublet
	4.33	Z (H3)	H3-H2 H3-H4	4.1 4.1	Triplet

between δ 3.5–3.8 ppm) (Fig. 3), but the corresponding unknown compounds could not be identified.

To verify if the proposed arabinaric acid and the other unknown chemical shifts were derived from side oxidation reactions of Ara during TEMPO reaction, NMR analyses were performed on the non-hydrolysed AX and ox-AX$^{1.0:2.6:0.4}$ samples. Only chemical shifts assigned to (residual) α-Ara, α-AraA, and β-Xyl were seen in the anomeric region of the ^{1}H-NMR spectrum of the non-hydrolysed ox-AX$^{1.0:2.6:0.4}$ (Fig. 4, full NMR spectra are shown in Fig. S4). Signals **a'**, **b'**, and **c'** in Fig. 4 were attributed to the H-1 of α-AraA based on our NMR results of ox-AX$^{1.0:2.6:0.4}$ hydrolysate (Figs. 2 and 3), and on literature showing that H-1 signals of t-GlcA in glucurono-arabinoxylans falls within the δ 5.0–5.6 ppm range (Munk et al., 2020; Yin, Lin, Nie, Cui, & Xie, 2012). Hence, these results indicate that the proposed arabinaric acid was likely formed from oxidation of the released Ara*f* during methanolysis and TFA hydrolysis of ox-AX$^{1.0:2.6:0.4}$, and that no other oxidation products than AraA are formed during TEMPO oxidation of AX. Generally, aldaric acids are produced by nitric acid oxidation of aldoses or by oxidation of the C1 terminal aldehyde group of an uronic acid (Hinton, Manley-Harris, Hardcastle, & Kiely, 2013; Mehtiö et al., 2016), although it has never been reported for the acid hydrolysis conditions used in our study.

Relatively low AraA signal intensities were noted in the ^{1}H-NMR spectrum of ox-AX$^{1.0:2.6:0.4}$ (Fig. 4B) in comparison to the corresponding Ara signal intensities in the ^{1}H-NMR spectrum of AX (Fig. 4A). However, accurate AraA quantitation could not be performed using these ^{1}H-NMR results due to the high viscosity of the ox-AX in comparison to AX.

3.4. Glycosidic linkages pattern of AX and ox-AX$^{1.0:2.6:0.4}$

GC–MS analyses of the partially-methylated alditol acetate (PMAA) forms derived from AX and carbodiimide/NaBD$_4$ carboxyl-reduced ox-AX$^{1.0:2.6:0.4}$ were performed to compare the substitution pattern over the xylan backbone between AX and ox-AX$^{1.0:2.6:0.4}$ samples. About 65.7 % (mol/mol) (4-Xyl*p*, mol/mol % of all Xyl residues in Table 4) of the β-(1→4)-xylan backbone in native AX was unsubstituted. Substitution of the xylan backbone occurred preferably as single-substitution at position *O*-3 of Xyl (24.7 %), but low amounts of double substitution at both *O*-2 and *O*-3 Xyl positions (5.8 %) and minor single-substitution at position *O*-2 of Xyl (2.3 %) also occurred in AX. These results are in agreement with previous studies (Gruppen, Hamer et al., 1992; Izydorczyk, 2009; Kormelink & Voragen, 1993; Saulnier et al., 2007).

Similar relative terminal-Xyl*p* amounts were found for AX and red-ox-AX$^{1.0:2.6:0.4}$ (Table 4), next to an increase of 1.8 % (mol/mol) in the relative amount of 2,4-linked Xyl*p*, likely due to debranching at position *O*-3 of the 2,3,4-Xyl*p* unit. The relative 4- and 3,4-Xyl*p* amounts present in the red-ox-AX$^{1.0:2.6:0.4}$ sample decreased 7.9 % and 8.6 %, respectively, whereas the 2,3,4-Xyl*p* amount concomitantly increased 14.9 % (mol/mol). This suggests that ox-AX$^{1.0:2.6:0.4}$ underwent undermethylation, which is substantiated by the increased 2,3,4-Xyl*p* content. Even though no conclusions can be drawn on the double substitution Xyl pattern due to undermethylation, still 20.2 % out of 27.0 % (mol/mol) expected single-substituted Xyl units (2,4- and 3,4-Xyl*p*) are present in the ox-AX$^{1.0:2.6:0.4}$. This suggests a DO of Ara higher than 75 % as derived from single-substituted xylan segments only. From this 75 %, 60

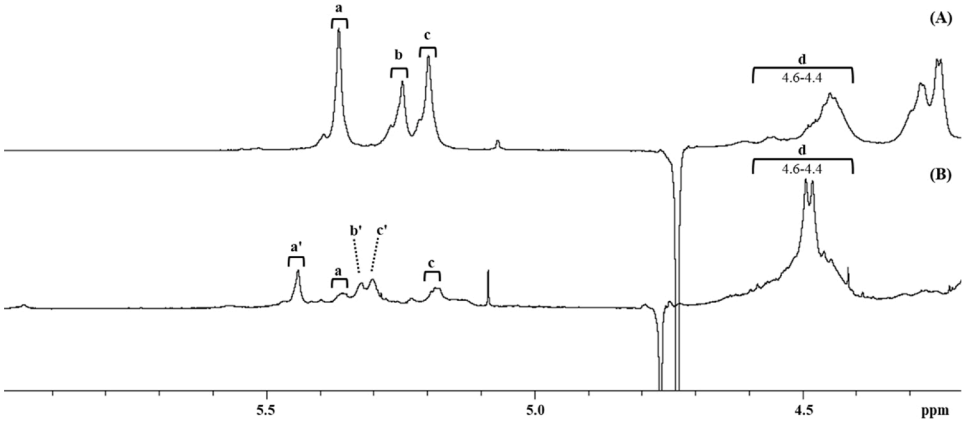

Fig. 4. ^{1}H-NMR spectra (600 MHz) of the anomeric region of the native AX (**A**) and ox-AX$^{1.0:2.6:0.4}$ (**B**) samples. H-1 signals of the α-Ara linked at positions *O*-3 of 3,4-Xyl (**a**), *O*-3 of 2,3,4-Xyl (**b**), and*O*-2 of 2,3,4-Xyl (**c**). **a'**, **b'**, and **c'** are assumed to be the corresponding signals derived from α-AraA, as the H-1 signals of t-GlcA in glucurono-arabinoxylans also falls within δ 5.0-5.6 ppm (Munk et al., 2020; Yin et al., 2012). **d** corresponds to the chemical shift range of the H-1 of the β-Xyl. Ara and Xyl-derived signal assignments were performed using previously published data (Bengtsson, Andersson, Westerlund, & Åman, 1992; Gruppen, Hoffmaann et al., 1992; Guo et al., 2019; Rondeau-Mouro, Ying, Ruellet, & Saulnier, 2011). Chemical shift range between δ 4.7-4.8 ppm is due to residual H_2O.

Table 4
Glycosidic linkage patterns of the of the native wheat AX and of the carboxyl-reduced ox-AX$^{1.0:2.6:0.4}$ (red-ox-AX$^{1.0:2.6:0.4}$) determined by methylation analysis.

Glycosidic linkage	% (mol/mol)	
	AX	Red-ox-AX$^{1.0:2.6:0.4}$ [a]
t-Xyl*p*	1.0 (1.4)	1.2 (1.4)
4-Xyl*p*	45.4 (65.7)	50.6 (57.8)
3,4-Xyl*p*	17.1 (24.7)	14.1 (16.1)
2,4-Xyl*p*	1.6 (2.3)	3.6 (4.1)
2,3,4-Xyl*p*	4.0 (5.8)	18.1 (20.7)
Total Xyl	**69.1 (65)***	**87.7 (85)***
t-Ara*f*	29.6	0.0
2-Ara*f*	0.8	0.0
3-Ara*f*	0.1	0.1
5-Ara*f*	0.4	0.1
3,5-Ara*f*	0.0	0.0
2,3,5-Ara*f*	0.0	0.0
Total Ara	**30.9 (35)***	**0.2 (-)***
t-AraA*f* [b]	–	9.3[b]
2-AraA*f* [b]	–	0.6[b]
2,3,5-AraA*f* [b]	–	2.1[b]
Total AraA*f*	–	**12.0 (15)***
Degree of branching (DB)[c]	38.6	61.6
t-Ara(A)/Xyl$_{subst}$	1.1	0.2

()values represent a relative mol % considering only Xyl residues.
()* values represent the relative mol % of sugar determined by HPAEC analysis of the hydrolysates.
[a] red-ox-AX$^{1.0:2.6:0.4}$ – ox-AX$^{1.0:2.6:0.4}$ was carboxyl-reduced with carbodiimide/NaBD$_4$ before being subjected to methylation.
[b] AraA moieties were measured as Ara but identified as AraA due to an increment of 2 in the *m/z* value of the EI-mass spectrum of Ara.
[c] DB was calculated as [Xyl$_{subst}$/Xyl$_{total}$], where Xyl$_{subst}$ is the sum of (2,4-Xyl + 3,4-Xyl + 2*2,3,4-Xyl) (Coelho, Rocha, Moreira, Domingues, & Coimbra, 2016).

% correspond to *O*-3 substituted Xyl, showing that ox-AX$^{1.0:2.6:0.4}$ was still mainly single-substituted at position *O*-3 of Xyl, similarly to AX. Considering that this 75 % single-substituted xylan segments should still be corrected for undermethylation, our results suggest that no major changes in the substitution pattern of the xylan backbone occurred.

Regarding Ara, this sugar was mainly found as t-Ara*f* (29.6 %, mol/mol) in AX (Table 4), indicating that the xylan backbone is mainly branched with single Ara units. Only low levels (< 0.8 %) of substituted Ara*f* residues (2-, 5-, and 3-Ara*f*) were observed, showing the presence of few oligomeric-Ara side chains in the AX native structure, which was also reported before (Izydorczyk, 2009; Kormelink & Voragen, 1993). Similarly, the carbodiimide/NaBD$_4$ carboxyl-reduced ox-AX$^{1.0:2.6:0.4}$ sample also displayed t-Ara*f* as main Ara derived residue. However, this residue was identified as t-AraA*f* instead of t-Ara*f* due to an increment of 2 in the *m/z* value relative to the PMAA derived from Ara, as a result of the AraA reduction to Ara with carbodiimide/NaBD$_4$ (Sims, Carnachan, Bell, & Hinkley, 2018; Taylor & Conrad, 1972). Carboxyl-reduced ox-AX$^{1.0:2.6:0.4}$ contained 9.3 % (mol/mol) of t-AraA*f* and low amounts of 2,3,5- and 2-AraA*f* moieties (2.1 and 0.6 %, respectively) (Table 4). Although the absolute Ara amount initially present in the ox-AX$^{1.0:2.6:0.4}$ sample increased from 2.1 % (w/w) (Table 2) to 9.7 % (w/w) (Table S1) in the carboxyl-reduced ox-AX$^{1.0:2.6:0.4}$ sample, the carboxyl-reduced ox-AX$^{1.0:2.6:0.4}$ still contained AraA (Fig. S2), demonstrating incomplete reduction of ox-AX$^{1.0:2.6:0.4}$. To reach complete reduction of ox-AX$^{1.0:2.6:0.4}$ and to obtain more accurate results, more than two reduction treatments using carbodiimide/NaBD$_4$ might be needed (Kamerling & Gerwig, 2007; Sims et al., 2018). Even though having incomplete reduction of ox-AX$^{1.0:2.6:0.4}$ and having noted some undermethylation of ox-AX$^{1.0:2.6:0.4}$, these results show that the single-substitution pattern of the xylan backbone of AX was basically conserved in ox-AX$^{1.0:2.6:0.4}$. This suggests that ox-AX$^{1.0:2.6:0.4}$ has a structure closely related to its native AX by comprising AraA side chains in place of Ara mainly at positions *O*-3 and/or *O*-2 of Xyl.

4. Conclusions

TEMPO:NaClO$_2$:NaOCl in a ratio of 1.0:2.6:0.4 per mol of C5-OH of Ara was the condition that allowed us to oxidize AX to an anionic polymer (arabinuronoxylan) with low level of polymer degradation, with minor effect on the xylan backbone and displaying charged side chains. These acidic side chains were identified to be arabinuronic acid (AraA) by COSY-NMR analysis of its monomeric oxidized-products, conferring an anionic nature to the polymer. Although an accurate AraA quantification could not be reached in our study and a low amount of Ara*f* was lost during oxidation, the conversion of Ara*f* towards AraA is rather complete. The glycosidic linkage analysis showed that >>75 % of the single-substituted β-(1→4)-xylan backbone was conserved in the ox-AX structure. Therefore, our results indicate that the ox-AX is an arabinuronoxylan mostly comprising AraA side chains, with a substituent distribution intimately related to its parental AX structure. This finding is rather interesting for structure elucidation of arabinoxylans by MS since AraA is heavier than the isomers Ara and Xyl, facilitating distinction of the Ara(A) side chains from the Xyl units by MS. Moreover, as AX are easily extracted and purified from cereals, and their level and pattern of branching with Ara can vary among AX from different sources, TEMPO-oxidation of various AX may yield arabinuronoxylans that display different functional properties, which is particularly valuable for further exploitation for food and/or biomedical applications.

Author contributions

All authors contributed to this study. Carolina O. Pandeirada, Hans-Gerd Janssen, Yvonne Westphal, and Henk A. Schols contributed to the conceptualization. Carolina O. Pandeirada developed the methodology and carried out the experiments. NMR experiments were performed by Carolina O. Pandeirada and Donny W. H. Merkx. Carolina O. Pandeirada and Donny W. H. Merkx performed the data curation and formal analysis. Carolina O. Pandeirada wrote the original draft. All authors were involved in critically reviewing all data and in writing the final manuscript. All authors read and approved the final manuscript to submission in Carbohydrate Polymers.

Appendix A. Supplementary data

Supplementary material related to this article can be found, in the online version, at doi:https://doi.org/10.1016/j.carbpol.2021.117781.

References

Benesi, A. J., Falzone, C. J., Banerjee, S., & Farber, G. K. (1994). NMR assignments for the aldopentoses. *Carbohydrate Research, 258*(C), 27–33. https://doi.org/10.1016/0008-6215(94)84072-5

Bengtsson, S., Andersson, R., Westerlund, E., & Åman, P. (1992). Content, structure and viscosity of soluble arabinoxylans in rye grain from several countries. *Journal of the Science of Food and Agriculture, 58*(3), 331–337. https://doi.org/10.1002/jsfa.2740580307

Börjesson, M., & Westman, G. (2016). Branching of hemicelluloses through an azetidinium salt ring-opening reaction. *Carbohydrate Research, 428*, 23–30. https://doi.org/10.1016/j.carres.2016.04.005

Bowman, M. J., Dien, B. S., O'Bryan, P. J., Sarath, G., & Cotta, M. A. (2011). Selective chemical oxidation and depolymerization of (Panicum virgatum L.) xylan with switchgrass oligosaccharide product analysis by mass spectrometry. *Rapid Communications in Mass Spectrometry, 25*(7), 941–950. https://doi.org/10.1002/rcm.4949

Bragd, P. L., Van Bekkum, H., & Besemer, A. C. (2004). TEMPO-mediated oxidation of polysaccharides: Survey of methods and applications. *Topics in Catalysis, 27*(1–4), 49–66. https://doi.org/10.1023/B:TOCA.0000013540.69309.46

Brückner, C. (2010). Nitroxide-catalyzed alcohol oxidations in organic synthesis. *Stable radicals: Fundamentals and applied aspects of odd-electron compounds* (pp. 433–460). John Wiley and Sons.

Chao, F.-C., Wu, M.-H., Chen, L.-C., Lin, H.-L., Liu, D.-Z., Ho, H.-O., et al. (2019). Preparation and characterization of chemically TEMPO-oxidized and mechanically disintegrated sacchachitin nanofibers (SCNF) for enhanced diabetic wound healing. *Carbohydrate Polymers*. , Article 115507. https://doi.org/10.1016/j.carbpol.2019.115507

Chatterjee, D., Halder, T., Pathak, N. P., Paul, A., Rajkamal, & Yadav, S. (2017). DAIB/TEMPO mediated synthesis of anomeric lactones from anomeric hydroxides. *Tetrahedron Letters, 58*(20), 1943–1946. https://doi.org/10.1016/j.tetlet.2017.04.019

Coelho, E., Rocha, M. A. M., Moreira, A. S. P., Domingues, M. R. M., & Coimbra, M. A. (2016). Revisiting the structural features of arabinoxylans from brewers' spent grain. *Carbohydrate Polymers, 139*, 167–176. https://doi.org/10.1016/j.carbpol.2015.12.006

Davis, N. J., & Flitsch, S. L. (1993). Selective oxidation of monosaccharide derivatives to uronic acids. *Tetrahedron Letters, 34*(7), 1181–1184. https://doi.org/10.1016/S0040-4039(00)77522-8

de Nooy, A. E. J., Besemer, A. C., & van Bekkum, H. (1994). Highly selective tempo mediated oxidation of primary alcohol groups in polysaccharides. *Recueil des Travaux Chimiques des Pays-Bas, 113*(3), 165–166. https://doi.org/10.1002/recl.19941130307

de Nooy, A. E. J., Besemer, A. C., & van Bekkum, H. (1995). Selective oxidation of primary alcohols mediated by nitroxyl radical in aqueous solution. Kinetics and mechanism. *Tetrahedron, 51*(29), 8023–8032. https://doi.org/10.1016/0040-4020(95)00417-7

De Ruiter, G. A., Schols, H. A., Voragen, A. G. J., & Rombouts, F. M. (1992). Carbohydrate analysis of water-soluble uronic acid-containing polysaccharides with high-performance anion-exchange chromatography using methanolysis combined with TFA hydrolysis is superior to four other methods. *Analytical Biochemistry, 207*(1), 176–185. https://doi.org/10.1016/0003-2697(92)90520-H

Dervilly, G., Saulnier, L., Roger, P., & Thibault, J. F. (2000). Isolation of homogeneous fractions from wheat water-soluble arabinoxylans. Influence of the structure on their macromolecular characteristics. *Journal of Agricultural and Food Chemistry, 48*(2), 270–278. https://doi.org/10.1021/jf990222k

Dervilly-Pinel, G., Thibault, J. F., & Saulnier, L. (2001). Experimental evidence for a semi-flexible conformation for arabinoxylans. *Carbohydrate Research, 330*(3), 365–372. https://doi.org/10.1016/S0008-6215(00)00300-1

Gruppen, H., Hamer, R. J., & Voragen, A. G. J. (1992). Water-unextractable cell wall material from wheat flour. 2. Fractionation of alkali-extracted polymers and comparison with water-extractable arabinoxylans. *Journal of Cereal Science, 16*(1), 53–67. https://doi.org/10.1016/S0733-5210(09)80079-9

Gruppen, H., Hoffmaann, R. A., Kormelink, F. J. M., Voragen, A. G. J., Kamerlin, J. P., & Vliegenthart, J. F. G. (1992). Characterisation by 1H NMR spectroscopy of enzymically derived oligosaccharides from alkali-extractable wheat-flour arabinoxylan. *Carbohydrate Research, 233*(C), 45–64. https://doi.org/10.1016/S0008-6215(00)90919-4

Guo, Q., Ai, L., & Cui, S. W. (2018). Methodology for structural analysis of polysaccharides. *Biobased polymers* (pp. 2510–3407). https://doi.org/10.1007/978-3-319-96370-9. Retrieved from.

Guo, R., Xu, Z., Wu, S., Li, X., Li, J., Hu, H., et al. (2019). Molecular properties and structural characterization of an alkaline extractable arabinoxylan from hull-less barley bran. *Carbohydrate Polymers, 218*, 250–260. https://doi.org/10.1016/j.carbpol.2019.04.093

Habibi, Y. (2014). Key advances in the chemical modification of nanocelluloses. *Chemical Society Reviews, 43*(5), 1519–1542. https://doi.org/10.1039/C3CS60204D

Hao, J., Wu, F., Tang, R., Sun, Y., Liu, D., & Zhang, Z. (2020). Preparation of 1,4-linked α-D-glucuronans from starch with 4-acetamide-TEMPO/NaClO2/NaClO system. *International Journal of Biological Macromolecules, 151*, 740–746. https://doi.org/10.1016/j.ijbiomac.2020.02.211

Hinton, M. R., Manley-Harris, M., Hardcastle, K. I., & Kiely, D. E. (2013). Pentaric acids and derivatives from nitric acid-oxidized pentoses. *Journal of Carbohydrate Chemistry, 32*(1), 68–85. https://doi.org/10.1080/07328303.2012.745550

Huang, J., Chen, W.-w., Hu, S., Gong, J.-Y., Lai, H.-W., Liu, P., et al. (2013). Biochemical activities of 6-carboxy β-chitin derived from squid pens. *Carbohydrate Polymers, 91*(1), 191–197. https://doi.org/10.1016/j.carbpol.2012.08.027

Isogai, A., Hänninen, T., Fujisawa, S., & Saito, T. (2018). Review: Catalytic oxidation of cellulose with nitroxyl radicals under aqueous conditions. *Progress in Polymer Science, 86*, 122–148. https://doi.org/10.1016/j.progpolymsci.2018.07.007

Izydorczyk, M. S. (2009). 23 - Arabinoxylans. In G. O. Phillips, & P. A. Williams (Eds.), *Handbook of hydrocolloids* (second edition, pp. 653–692). Woodhead Publishing.

Izydorczyk, M. S., & Biliaderis, C. G. (1993). Structural heterogeneity of wheat endosperm arabinoxylans. *Cereal Chemistry, 70*(6), 641–646.

Izydorczyk, M. S., & Biliaderis, C. G. (1995). Cereal arabinoxylans: Advances in structure and physicochemical properties. *Carbohydrate Polymers, 28*(1), 33–48. https://doi.org/10.1016/0144-8617(95)00077-1

Kamerling, J. P., & Gerwig, G. J. (2007). 2.01 - Strategies for the structural analysis of carbohydrates. In H. Kamerling (Ed.), *Comprehensive glycoscience* (pp. 1–68). Oxford: Elsevier.

Kiemle, D. J., Stipanovic, A. J., & Mayo, K. E. (2004). Proton NMR methods in the compositional characterization of polysaccharides. *ACS Symposium Series, 864*, 122–139.

Kormelink, F. J. M., & Voragen, A. G. J. (1993). Degradation of different [(glucurono) arabino]xylans by a combination of purified xylan-degrading enzymes. *Applied Microbiology and Biotechnology, 38*(5), 688–695. https://doi.org/10.1007/BF00182811

Lin, C., Zeng, T., Wang, Q., Huang, L., Ni, Y., Huang, F., et al. (2019). Effects of the conditions of the TEMPO/NaBr/NaClO System on carboxyl groups, degree of polymerization, and yield of the oxidized cellulose. *BioResources, 13*(3), 5965–5975. https://doi.org/10.15376/biores.13.3.5965-597

Malz, F., & Jancke, H. (2005). Validation of quantitative NMR. *Journal of Pharmaceutical and Biomedical Analysis, 38*(5 SPEC. ISS), 813–823. https://doi.org/10.1016/j.jpba.2005.01.043

Mehtiö, T., Toivari, M., Wiebe, M. G., Harlin, A., Penttilä, M., & Koivula, A. (2016). Production and applications of carbohydrate-derived sugar acids as generic biobased chemicals. *Critical Reviews in Biotechnology, 36*(5), 904–916. https://doi.org/10.3109/07388551.2015.1060189

Mendoza, D. J., Browne, C., Raghuwanshi, V. S., Simon, G. P., & Garnier, G. (2019). One-shot TEMPO-periodate oxidation of native cellulose. *Carbohydrate Polymers, 226*, Article 115292. https://doi.org/10.1016/j.carbpol.2019.115292

Meng, Q., Fu, S., & Lucia, L. A. (2016). The role of heteropolysaccharides in developing oxidized cellulose nanofibrils. *Carbohydrate Polymers, 144*, 187–195. https://doi.org/10.1016/j.carbpol.2016.02.058

Merkx, D. W. H., Westphal, Y., van Velzen, E. J. J., Thakoer, K. V., de Roo, N., & van Duynhoven, J. P. M. (2018). Quantification of food polysaccharide mixtures by 1H NMR. *Carbohydrate Polymers, 179*, 379–385. https://doi.org/10.1016/j.carbpol.2017.09.074

Munk, L., Muschiol, J., Li, K., Liu, M., Perzon, A., Meier, S., et al. (2020). Selective enzymatic release and gel formation by cross-linking of feruloylated glucurono-arabinoxylan from corn bran. *ACS Sustainable Chemistry & Engineering, 8*(22), 8164–8174. https://doi.org/10.1021/acssuschemeng.0c00663

Nunes, C., Silva, L., Fernandes, A. P., Guiné, R. P. F., Domingues, M. R. M., & Coimbra, M. A. (2012). Occurrence of cellobiose residues directly linked to galacturonic acid in pectic polysaccharides. *Carbohydrate Polymers, 87*(1), 620–626. https://doi.org/10.1016/j.carbpol.2011.08.027

Pandeirada, C. O., Maricato, É., Ferreira, S. S., Correia, V. G., Pinheiro, B. A., Evtuguin, D. V., et al. (2019). Structural analysis and potential immunostimulatory activity of Nannochloropsis oculata polysaccharides. *Carbohydrate Polymers, 222*. https://doi.org/10.1016/j.carbpol.2019.06.001

Parikka, K., Nikkilä, I., Pitkänen, L., Ghafar, A., Sontag-Strohm, T., & Tenkanen, M. (2017). Laccase/TEMPO oxidation in the production of mechanically strong arabinoxylan and glucomannan aerogels. *Carbohydrate Polymers, 175*, 377–386. https://doi.org/10.1016/j.carbpol.2017.07.074

Perez, S. (2018). *Symbolic representation of monosaccharides in the age of glycobiology*.

Perlin, A. S. (1951). Structure of the soluble pentosans of wheat flours. *Cereal Chemistry, 28*, 382–393.

Pierre, G., Punta, C., Delattre, C., Melone, L., Dubessay, P., Fiorati, A., et al. (2017). TEMPO-mediated oxidation of polysaccharides: An ongoing story. *Carbohydrate Polymers, 165*, 71–85. https://doi.org/10.1016/j.carbpol.2017.02.028

Rejzek, M., Mukhopadhyay, B., Wenzel, C. Q., Lam, J. S., & Field, R. A. (2007). Direct oxidation of sugar nucleotides to the corresponding uronic acids: TEMPO and platinum-based procedures. *Carbohydrate Research, 342*(3-4), 460–466. https://doi.org/10.1016/j.carres.2006.10.016

Rondeau-Mouro, C., Ying, R., Ruellet, J., & Saulnier, L. (2011). Structure and organization within films of arabinoxylans extracted from wheat flour as revealed by various NMR spectroscopic methods. *Magnetic Resonance in Chemistry, 49*(SUPPL. 1), S85–S92. https://doi.org/10.1002/mrc.2852

Saito, T., Hirota, M., Tamura, N., & Isogai, A. (2010). Oxidation of bleached wood pulp by TEMPO/NaClO/NaClO2 system: Effect of the oxidation conditions on carboxylate content and degree of polymerization. *Journal of Wood Science, 56*(3), 227–232. https://doi.org/10.1007/s10086-009-1092-7

Sakakibara, C. N., Sierakowski, M. R., Lucyszyn, N., & de Freitas, R. A. (2016). TEMPO-mediated oxidation on galactomannan: Gal/man ratio and chain flexibility dependence. *Carbohydrate Polymers, 153*, 371–378. https://doi.org/10.1016/j.carbpol.2016.07.114

Saulnier, L., Sado, P.-E., Branlard, G., Charmet, G., & Guillon, F. (2007). Wheat arabinoxylans: Exploiting variation in amount and composition to develop enhanced varieties. *Journal of Cereal Science, 46*(3), 261–281. https://doi.org/10.1016/j.jcs.2007.06.014

Shibata, I., & Isogai, A. (2003). Depolymerization of cellouronic acid during TEMPO-mediated oxidation. *Cellulose, 10*(2), 151–158. https://doi.org/10.1023/A:1024051514026

Sierakowski, M. R., Milas, M., Desbrières, J., & Rinaudo, M. (2000). Specific modifications of galactomannans. *Carbohydrate Polymers, 42*(1), 51–57. https://doi.org/10.1016/S0144-8617(99)00137-X

Sims, I. M., Carnachan, S. M., Bell, T. J., & Hinkley, S. F. R. (2018). Methylation analysis of polysaccharides: Technical advice. *Carbohydrate Polymers, 188*, 1–7. https://doi.org/10.1016/j.carbpol.2017.12.075

Spier, V. C., Sierakowski, M. R., Reed, W. F., & de Freitas, R. A. (2017). Polysaccharide depolymerization from TEMPO-catalysis: Effect of TEMPO concentration. *Carbohydrate Polymers, 170*, 140–147. https://doi.org/10.1016/j.carbpol.2017.04.064

Sun, P., Frommhagen, M., Kleine Haar, M., van Erven, G., Bakx, E. J., van Berkel, W. J. H., et al. (2020). Mass spectrometric fragmentation patterns discriminate C1- and C4-oxidised cello-oligosaccharides from their non-oxidised and reduced forms. *Carbohydrate Polymers.* , Article 115917. https://doi.org/10.1016/j.carbpol.2020.115917

Sundar Raj, A. A., Rubila, S., Jayabalan, R., & Ranganathan, T. V. (2012). A review on pectin: Chemistry due to general properties of pectin and its pharmaceutical uses. *Open Access Scientific Reports, 1*(550), 1–4. https://doi.org/10.4172/scientificreports.550

Takeda, T., Miller, J. G., & Fry, S. C. (2008). Anionic derivatives of xyloglucan function as acceptor but not donor substrates for xyloglucan endotransglucosylase activity. *Planta, 227*(4), 893–905. https://doi.org/10.1007/s00425-007-0665-1

Tamura, N., Hirota, M., Saito, T., & Isogai, A. (2010). Oxidation of curdlan and other polysaccharides by 4-acetamide-TEMPO/NaClO/NaClO2 under acid conditions. *Carbohydrate Polymers, 81*(3), 592–598. https://doi.org/10.1016/j.carbpol.2010.03.016

Tamura, N., Wada, M., & Isogai, A. (2009). TEMPO-mediated oxidation of (1→3)-β-d-glucans. *Carbohydrate Polymers, 77*(2), 300–305. https://doi.org/10.1016/j.carbpol.2008.12.040

Tanaka, R., Saito, T., & Isogai, A. (2012). Cellulose nanofibrils prepared from softwood cellulose by TEMPO/NaClO/NaClO2 systems in water at pH 4.8 or 6.8. *International Journal of Biological Macromolecules, 51*(3), 228–234. https://doi.org/10.1016/j.ijbiomac.2012.05.016

Taylor, R. L., & Conrad, H. E. (1972). Stoichiometric depolymerization of polyuronides and glycosaminoglycuronans to monosaccharides following reduction of their carbodiimide-activated carboxyl group. *Biochemistry, 11*(8), 1383–1388. https://doi.org/10.1021/bi00758a009

ter Haar, R., Timmermans, J. W., Slaghek, T. M., Van Dongen, F. E. M., Schols, H. A., & Gruppen, H. (2010). TEMPO oxidation of gelatinized potato starch results in acid resistant blocks of glucuronic acid moieties. *Carbohydrate Polymers, 81*(4), 830–838. https://doi.org/10.1016/j.carbpol.2010.03.060

Tojo, G., & Fernández, M. (2007). Oxidation of primary alcohols to carboxylic acids: A guide to current common practice. *Basic reactions in organic synthesis*. https://doi.org/10.1007/0-387-35432-8

Wu, J., & Serianni, A. S. (1991). d-Penturonic acids: Solution studies of stable-isotopically enriched compounds by 1H- and 13C-n.m.r. spectroscopy. *Carbohydrate Research, 210*, 51–70. https://doi.org/10.1016/0008-6215(91)80112-Z

Yin, J. Y., Lin, H. X., Nie, S. P., Cui, S. W., & Xie, M. Y. (2012). Methylation and 2D NMR analysis of arabinoxylan from the seeds of Plantago asiatica L. *Carbohydrate Polymers, 88*(4), 1395–1401. https://doi.org/10.1016/j.carbpol.2012.02.025